



# The transcription factor NKX1-2 promotes adipogenesis and may contribute to a balance between adipocyte and osteoblast differentiation

Received for publication, February 11, 2019, and in revised form, October 4, 2019. Published, Papers in Press, October 15, 2019, DOI 10.1074/jbc.RA119.007967

Noah Chen<sup>‡</sup>,  Rebecca L. Schill<sup>§</sup>, Michael O'Donnell<sup>‡</sup>, Kevin Xu<sup>‡</sup>,  Devika P. Bagchi<sup>§</sup>, Ormond A. MacDougald<sup>‡§</sup>,  Ronald J. Koenig<sup>‡1</sup>, and Bin Xu<sup>‡2</sup>

From the <sup>‡</sup>Division of Metabolism, Endocrinology and Diabetes, Department of Internal Medicine and <sup>§</sup>Department of Molecular and Integrative Physiology, University of Michigan Medical School, Ann Arbor, Michigan 48109

Edited by Qi-Qun Tang

Although adipogenesis is mainly controlled by a small number of master transcription factors, including CCAAT/enhancer-binding protein family members and peroxisome proliferator-activated receptor  $\gamma$  (PPAR $\gamma$ ), other transcription factors also are involved in this process. Thyroid cancer cells expressing a paired box 8 (PAX8)–PPAR $\gamma$  fusion oncogene trans-differentiate into adipocyte-like cells in the presence of the PPAR $\gamma$  ligand pioglitazone, but this trans-differentiation is inhibited by the transcription factor NK2 homeobox 1 (NKX2-1). Here, we tested whether NKX family members may play a role also in normal adipogenesis. Using quantitative RT-PCR (RT-qPCR), we examined the expression of all 14 NKX family members during 3T3-L1 adipocyte differentiation. We found that most NKX members, including NKX2-1, are expressed at very low levels throughout differentiation. However, mRNA and protein expression of a related family member, NKX1-2, was induced during adipocyte differentiation. NKX1-2 also was up-regulated in cultured murine ear mesenchymal stem cells (EMSCs) during adipogenesis. Importantly, shRNA-mediated NKX1-2 knock-down in 3T3-L1 preadipocytes or EMSCs almost completely blocked adipocyte differentiation. Furthermore, NKX1-2 over-expression promoted differentiation of the ST2 bone marrow-derived mesenchymal precursor cell line into adipocytes. Additional findings suggested that NKX1-2 promotes adipogenesis by inhibiting expression of the antiadipogenic protein COUP transcription factor II. Bone marrow mesenchymal precursor cells can differentiate into adipocytes or osteoblasts, and we found that NKX1-2 both promotes ST2 cell adipogenesis and inhibits their osteoblastogenic differentiation. These results support a role for NKX1-2 in promoting adipogenesis and possibly in regulating the balance between adipocyte and osteoblast differentiation of bone marrow mesenchymal precursor cells.

Obesity is associated with premature death due to its link to type 2 diabetes, hypertension, cardiovascular disease, stroke, and certain cancers (1–3). Adipose tissue plays a central role in energy homeostasis and is composed of mesenchymal stem cells, vascular cells, preadipocytes, and mature fat cells. White adipose tissue, which expands in obesity, is specialized to store energy in the form of lipid, whereas brown and beige adipose cells primarily serve a thermogenic function (4). Adipogenesis has been studied extensively *in vitro*, in particular using the murine 3T3-L1 preadipocyte line that can be induced to differentiate into mature white adipocytes by exposure to an adipogenic mixture consisting of the synthetic glucocorticoid dexamethasone, insulin, the phosphodiesterase inhibitor isobutylmethylxanthine, and fetal bovine serum (FBS)<sup>3</sup> (5–8).

This well-studied adipocyte differentiation is controlled by a tightly regulated cascade of key transcription factors (TFs), including CCAAT/enhancer-binding protein (C/EBP) family members (C/EBP $\alpha$ , C/EBP $\beta$ , and C/EBP $\delta$ ) and the nuclear receptor peroxisome proliferator-activated receptor  $\gamma$  (PPAR $\gamma$ ), which have been shown both *in vitro* and *in vivo* to be the master regulators of adipogenesis (9). In addition, other TFs and cofactors, such as KLFs (10, 11), STAT5 (12, 13), PBX1 (14), Krox20 (15), AP1 (16, 17), ATFs (18), GATA2/3 (19, 20), TAF8 (21), and Mediator subunits (MED1, MED14, and NED23) (22–24), have been reported to be involved in regulating either adipocyte commitment or differentiation in cell line and/or mouse models. Recent studies using ChIP and DNase hypersensitivity mapping have provided substantial insight into the specific gene expression and epigenetic changes that underlie adipogenesis (25–34). However, due to the diversity of factors and mechanisms involved in adipocyte differentiation, the full com-

The authors declare that they have no conflicts of interest with the contents of this article.

This article contains Figs. S1 and S2 and Table S1.

<sup>1</sup> To whom correspondence may be addressed: Division of Metabolism, Endocrinology and Diabetes, University of Michigan Medical Center, Ann Arbor, MI 48109-5678. Tel.: 734-647-2883; Fax: 734-936-6684; E-mail: rkoenig@umich.

<sup>2</sup> To whom correspondence may be addressed: Division of Metabolism, Endocrinology and Diabetes, University of Michigan Medical Center, Ann Arbor, MI 48109-5678. Tel.: 734-647-2883; Fax: 734-936-6684; E-mail: bxu@umich.edu.

<sup>3</sup> The abbreviations used are: FBS, fetal bovine serum; PPAR $\gamma$ , peroxisome proliferator-activated receptor  $\gamma$ ; NKX2-1, NK2 homeobox 1; PAX8, paired box 8; qPCR, quantitative PCR; EMSC, ear mesenchymal stem cell; COUP, chicken ovalbumin upstream promoter; TF, transcription factor; C/EBP, CCAAT/enhancer-binding protein; HD, homeodomain; KLF, Kruppel-like factor; ATF, Activating transcription factor; TTF-1, thyroid transcription factor 1; PFPF, PAX8–PPAR $\gamma$  fusion protein; MDI, 3-isobutyl-1-methylxanthine, dexamethasone and insulin; ORO, Oil Red O; EV, empty vector; HSL, hormone-sensitive lipase; SMRT, silencing mediator of retinoic acid and thyroid hormone receptor; GSK3, glycogen synthase kinase 3; bFGF, basic fibroblast growth factor; GAPDH, glyceraldehyde-3-phosphate dehydrogenase; ANOVA, analysis of variance; shControl, control shRNA; Rosi, rosiglitazone.

plement of key transcriptional regulators that orchestrate adipogenesis remains to be elucidated.

The NKX family of homeodomain (HD)-containing TFs includes numerous members that display diverse functions in cell fate determination, development (especially of the nervous system), and tumorigenesis (35–37). For example, NKX1-2, which is the focus of this study, is expressed early in development in neuromesodermal progenitor cells and contributes to the formation of all three germ layers (38–40). NKX1-1/Sax2 is expressed predominantly in the brainstem, through which it plays an important role in whole-animal energy homeostasis and adiposity (41). NKX2-2 is required for cell patterning in the ventral neural tube and pancreatic islet  $\beta$ -cell specification (36, 42, 43). NKX2-5 plays important roles in cardiac and thyroid development (44). NKX5-1 plays a role in neuronal cell-type specification and is required for development of the inner ear and hypothalamus (45, 46). NKX6-1 is required for pancreatic  $\beta$ -cell development (47, 48). NKX6-2 regulates axon–glia interactions, and its mutation causes a form of spastic ataxia (49). Finally, NKX2-1 (also called thyroid transcription factor 1 (TTF-1)) is essential for development of the thyroid, lung, and brain (50).

As noted above, PPAR $\gamma$  is a master regulator of adipogenesis. Although PPAR $\gamma$  is expressed at very low levels in the normal thyroid and has no known function in normal thyroid biology (51), a subset of thyroid cancers is caused by a chromosomal translocation that fuses the genes *PAX8* and *PPARG*, resulting in expression of an oncogenic PAX8–PPAR $\gamma$  fusion protein (PPFP) (52). We previously found that pioglitazone, a synthetic agonist ligand for PPAR $\gamma$ , also binds to PPFP and turns it into a strongly PPAR $\gamma$ -like protein, resulting in adipogenic trans-differentiation of PPFP-expressing thyroid cancer cells (53). We also found that NKX2-1 physically interacts with PPFP and inhibits PPFP/pioglitazone-mediated adipogenic trans-differentiation (54). These data led us to test whether NKX family members may play a role in normal adipogenesis. We found that the transcriptional repressor NKX1-2 promotes the differentiation of preadipocytes into adipocytes, at least in part by repressing the expression of the negative adipogenic regulator chicken ovalbumin upstream promoter (COUP)-TF II (55, 56). In addition, not only does NKX1-2 promote the adipogenic differentiation of ST2 cells, a bone marrow–derived mesenchymal precursor cell line, it also inhibits the differentiation of those cells into osteoblasts. Overall, our data suggest a novel role for NKX1-2 in adipogenesis and possibly in bone homeostasis.

## Results

### The homeodomain transcription factor NKX2-1/TTF-1 inhibits adipogenesis of 3T3-L1 cells

We recently found that thyroid cancer cells expressing the PAX8–PPAR $\gamma$  fusion oncogene trans-differentiate into adipocyte-like cells in the presence of the PPAR $\gamma$  agonist ligand pioglitazone, but that this trans-differentiation is inhibited by the homeodomain TF NKX2-1/TTF-1 (54). This led us to hypothesize that NKX family members may play a role in normal adipogenesis. To begin to test this hypothesis, we stably

overexpressed NKX2-1 in 3T3-L1 preadipocytes and found that this inhibits differentiation to mature adipocytes, as indicated by reduced formation of lipid droplets and decreased expression of markers of mature adipocytes, including PPAR $\gamma$ , C/EBP $\alpha$ , and FABP4 (Fig. S1). However, we found that, prior to and throughout differentiation, endogenous NKX2-1 is expressed at negligible levels in 3T3-L1 cells (Fig. 1), calling into question the physiological relevance of the overexpression data. This led us to test whether other NKX family members may play a role in adipogenesis.

### NKX1-2 is induced during adipocyte differentiation

The endogenous expression of all 14 NKX family members was evaluated by reverse transcription-quantitative PCR (RT-qPCR) during 3T3-L1 preadipocyte differentiation. We found that most *Nkx* genes, including *Nkx2-1*, are expressed at very low levels throughout differentiation. However, the related family member *Nkx1-2* is induced during adipocyte differentiation at both the mRNA and protein levels (Fig. 1, A and B).

### NKX1-2 knockdown inhibits adipocyte differentiation

We next evaluated the effect of NKX1-2 depletion on adipogenesis. Two independent shRNAs targeting different regions of *Nkx1-2* (Fig. 2A) were used to knock down endogenous *Nkx1-2* at both the protein and RNA levels in 3T3-L1 preadipocytes (Fig. 2, C and D). Importantly, knockdown of endogenous NKX1-2 almost completely blocked adipocyte differentiation as indicated by decreased Oil Red O (ORO) staining of neutral lipid (Fig. 2B) and reduced protein and/or RNA expression of adipocyte markers PPAR $\gamma$ , C/EBP $\alpha$ , FABP4, and adiponectin (Figs. 2, C and D, and S2, A and B). Furthermore, knockdown of endogenous NKX1-2 using the same shRNAs also inhibited the differentiation of cultured murine ear mesenchymal stem cells (EMSCs) into mature adipocytes, as demonstrated by reduced ORO staining (Fig. 3A) and reduced expression of PPAR $\gamma$ , C/EBP $\alpha$ , and FABP4 (Fig. 3B).

### NKX1-2 overexpression promotes differentiation of adipocyte precursor ST2 cells

We next asked whether NKX1-2 overexpression could promote adipogenesis. Interestingly, overexpression of NKX1-2 in 3T3-L1 preadipocytes (pMSCV-Nkx1-2) inhibited their proliferation compared with controls (pMSCV empty vector (pMSCV-EV)) (data not shown); thus, we were unable to study their ability to differentiate. In contrast, overexpression of NKX1-2 did not impair the growth rate of ST2 mesenchymal precursor cells (data not shown). Importantly, overexpression of NKX1-2 in ST2 cells (Fig. 4A) promoted their differentiation into adipocytes, as evidenced by increases in ORO staining (Fig. 4B) and the mRNA expression of the adipocyte markers PPAR $\gamma$ , C/EBP $\alpha$ , FABP4, adiponectin, resistin, and hormone-sensitive lipase (HSL) (Fig. 4C). Overexpressing NKX1-2 in ST2 cells significantly increased the RNA expression of PPAR $\gamma$  and C/EBP $\alpha$  even at Day 0 before hormone inductions. Overexpression of NKX1-2 also increased the protein expression of PPAR $\gamma$ , FABP4, and the p42 isoform of C/EBP $\alpha$  but not the p30 isoform (Fig. 4D). The p42 isoform of C/EBP $\alpha$  has been shown to be sufficient to trigger the differentiation program of 3T3-L1

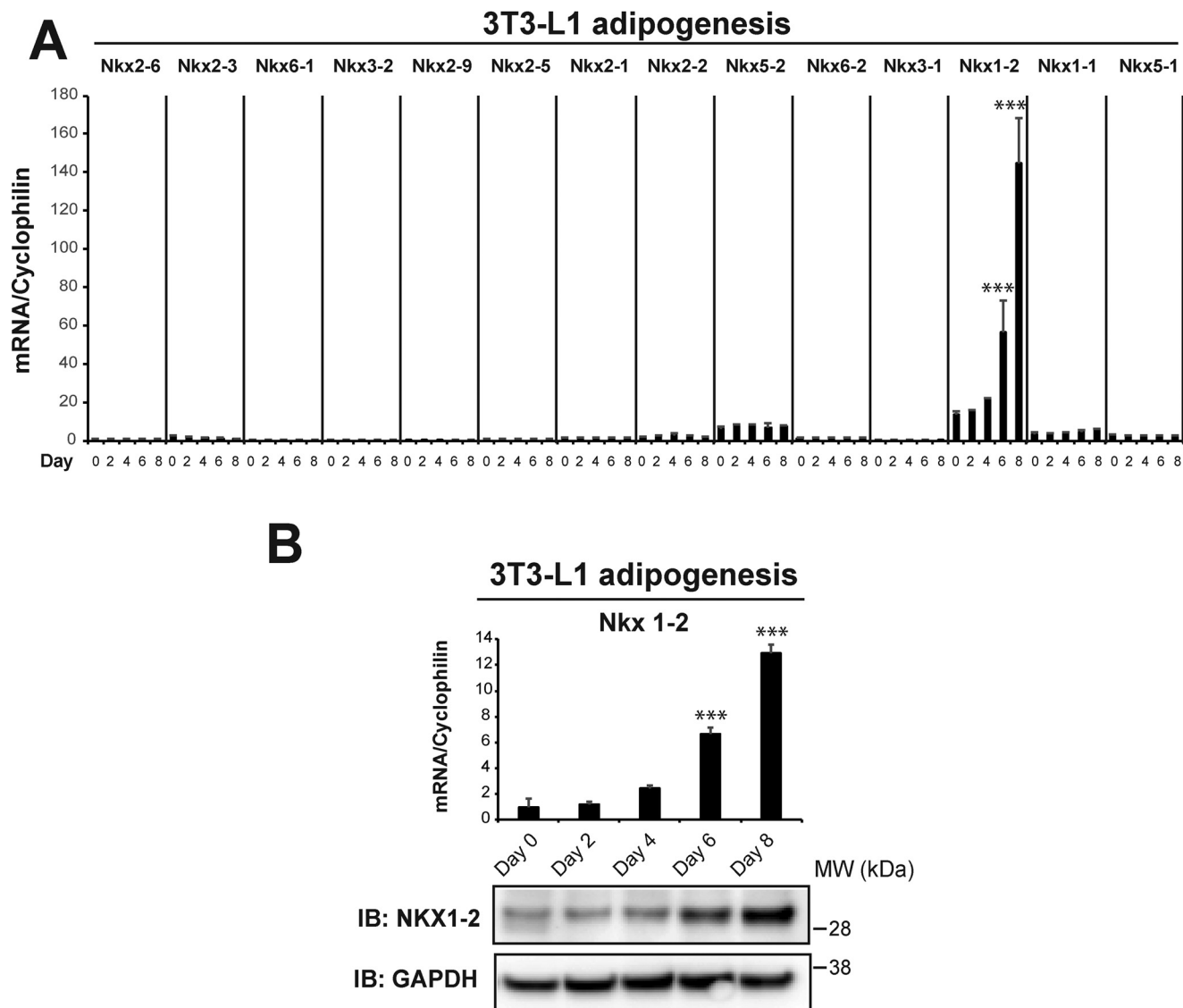


**Figure 1. NKX1-2 is induced during adipocyte differentiation.** A, 3T3-L1 preadipocytes were induced to differentiate with MDI and total RNA was isolated at the times indicated (Day 0 is the day of addition of the hormone mixture). RT-qPCR was then performed to measure the mRNA expression level of each Nkx family member at each time point. RNA expression was normalized to cyclophilin mRNA, and the expression is given relative to the RNA level of Nkx2-6 at Day 0 set at 1. B, upper panel, an independent experiment to analyze Nkx1-2 expression during 3T3-L1 cell adipocyte differentiation using the same conditions as in A. RNA expression was normalized to cyclophilin mRNA, and the expression is given relative to the RNA level of Nkx1-2 at Day 0 set at 1. B, lower panel, immunoblot (IB) for NKX1-2 and GAPDH as a loading control. A and B, upper panel, data are given as the mean  $\pm$  S.D. (error bars) from triplicate samples. Statistical significance was evaluated with an ANOVA followed by Dunnett's test compared with Day 0 expression level as control for each gene: \*\*\*,  $p < 0.001$ . These results are representative of three independent experiments.

preadipocytes (57, 58). Overall, these data support the hypothesis that NKX1-2 is a novel proadipogenic TF that up-regulates the expression of the adipocyte master TFs PPAR $\gamma$  and C/EBP $\alpha$  and their downstream targets FABP4, adiponectin, resistin, and HSL.

**NKX1-2 promotes adipocyte differentiation by inhibiting COUP-TF II expression, and the HD of NKX1-2 is required for this inhibition**

The orphan nuclear receptor COUP-TF II (Nr2f2) is expressed in adipose tissue *in vivo* and declines during differentiation (56). Two key studies revealed that COUP-TF II is an endogenous antiadipogenic factor that acts downstream of hedgehog signaling by association with GATA2 to repress

C/EBP $\alpha$  (56) and/or downstream of Wnt/ $\beta$ -catenin signaling by recruitment of the SMRT corepressor complex to the *PPARG* gene (55). Given that overexpression of NKX1-2 up-regulates the expression of PPAR $\gamma$  and C/EBP $\alpha$  and that NKX1-2 is a transcriptional repressor (40), we tested whether the NKX1-2 proadipogenic effect is mediated by inhibition of COUP-TF II expression. Indeed, overexpressing NKX1-2 inhibited the mRNA and protein expression of COUP-TF II during ST2 cell adipogenic differentiation (Fig. 5A). Conversely, knockdown of endogenous NKX1-2 in 3T3-L1 preadipocytes increased the expression of COUP-TF II during adipogenesis (Fig. 5B). These results suggest that NKX1-2 promotes adipocyte differentiation at least in part by inhibiting the expression of the antiadipogenic factor COUP-TF II.

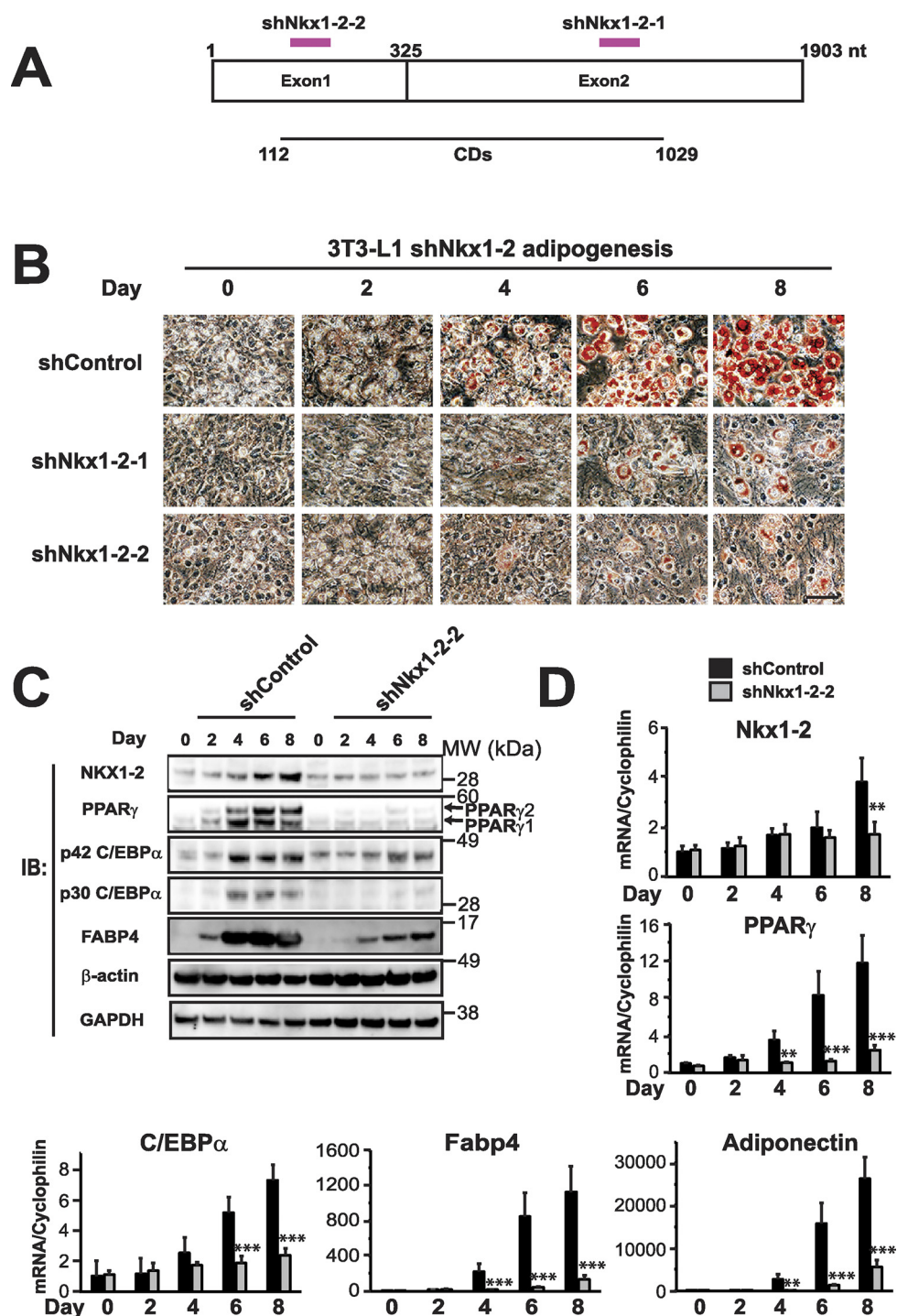


**Figure 2. Depletion of endogenous NKX1-2 inhibits 3T3-L1 adipocyte differentiation.** *A*, two shRNAs targeting different regions of endogenous murine Nkx1-2 mRNA were expressed from a lentiviral vector. *CDs*, protein-coding sequence. *B*, 3T3-L1 preadipocytes were infected with lentiviruses expressing either the shControl or one of two shRNAs directed against mouse Nkx1-2 (shNkx1-2-1 or shNkx1-2-2). Preadipocytes were induced to differentiate with MDI. During the time course of differentiation indicated, cells were stained with ORO to assess neutral lipid accumulation. Day 0 is the day of addition of the hormone mixture. All panels are the same magnification; a 100- $\mu$ m scale bar is shown in the lower right panel. *C*, 3T3-L1 preadipocytes expressing either shControl or shNkx1-2-2 were induced to differentiate as described in *B*. Cells were harvested, and immunoblotting (IB) was performed at the time course indicated.  $\beta$ -Actin and GAPDH served as loading controls. Results with shNkx1-2-1 are highly similar and are therefore presented in Fig. S2. *D*, time course of mRNA expression for Nkx1-2, PPAR $\gamma$ , C/EBP $\alpha$ , FABP4, and adiponectin analyzed by RT-qPCR. Data were normalized to cyclophilin, and the expression of each gene at Day 0 in shControl was set at 1. Data are given as the mean  $\pm$  S.D. (error bars) of triplicate samples. Statistical significance versus shControl at each time point was evaluated with the Student's *t* test: \*\*,  $p < 0.01$  and \*\*\*,  $p < 0.001$ . These results are representative of three independent experiments.

To further test this hypothesis, we knocked down endogenous COUP-TF II in control shRNA (shControl) or shNkx1-2 3T3-L1 preadipocytes. As expected, in shControl cells (shCon-

trol 1), knockdown of COUP-TF II promoted adipocyte differentiation as shown by increased ORO staining (Fig. 5C, top panels) and increased expression of PPAR $\gamma$ , FABP4, and

## NKX1-2 regulates adipogenesis

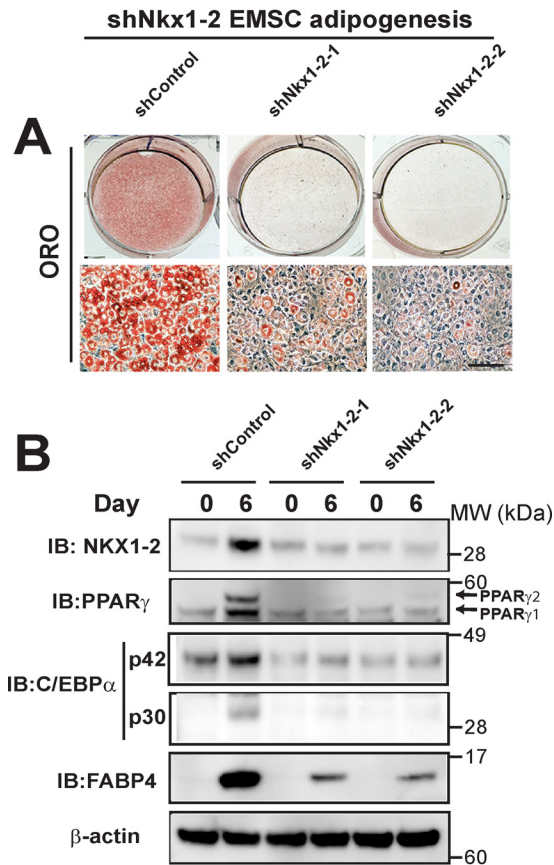


**Figure 3. Depletion of endogenous NKX1-2 inhibits cultured murine EMSC adipocyte differentiation.** A, cultured EMSCs expressing shControl, shNkx1-2-1, or shNkx1-2-2 were induced to differentiate into adipocytes with the hormone mixture MDI. At the end of differentiation (Day 6), cells were stained with ORO to assess neutral lipid accumulation. All micrographs are the same magnification; a 100- $\mu$ m scale bar is shown in the lower right panel. B, immunoblotting (IB) for NKX1-2 protein and the mature adipocyte marker proteins PPAR $\gamma$ , C/EBP $\alpha$ , or FABP4 was performed on lysates harvested at Day 0 before differentiation and Day 6 at the end of differentiation.  $\beta$ -Actin served as a loading control. These results are representative of three independent experiments.

C/EBP $\alpha$  at the protein and mRNA levels (Fig. 5, D and E, lanes 2 versus lanes 1). Importantly, in shNkx1-2 cells, knockdown of COUP-TF II partially reversed the repression of adipocyte differentiation caused by NKX1-2 knockdown, as indicated by increased ORO staining (Fig. 5C, bottom panels) and increased expression of PPAR $\gamma$ , FABP4, and C/EBP $\alpha$  (Fig. 5, D and E, lanes 4 versus lanes 3). This supports the hypothesis that the adipogenic action of NKX1-2 is mediated by regulation of COUP-TF II expression. The fact that shCOUP-TF II only partially reversed shNkx1-2-mediated repression of adipocyte differentiation could reflect the fact that COUP-TF II knockdown was incomplete or could indicate that additional mechanisms also contribute to the action of NKX1-2.

NKX1-2 is a member of the HD-containing family of TFs. In the majority of cases, the DNA-binding specificity of HD-containing proteins resides exclusively within the HD itself (59), although in some cases, other domains may cooperate with the HD (60, 61). Therefore, we hypothesized that the HD of NKX1-2 plays an important role in its regulation of adipogenesis. To test this hypothesis, we expressed an HD-deleted mutant of NKX1-2 from the retroviral vector pMSCV

(pMSCV-Nkx1-2HDD) and transduced it in parallel with the empty vector (pMSCV-EV) and intact NKX1-2 (pMSCV-Nkx1-2) into ST2 cells (Fig. 6, A and B). As expected, overexpression of full-length NKX1-2 significantly increased ST2 cell differentiation into mature adipocytes, as indicated by increased ORO staining (Fig. 6C) and increased expressions of PPAR $\gamma$ , C/EBP $\alpha$ , and FABP4 at the RNA and protein levels (Fig. 6, D and E). In contrast, HD-deleted NKX1-2 (NKX1-2HDD) was unable to increase ST2 cell adipogenic differentiation. Strikingly, NKX1-2HDD also no longer inhibited the expression of the antiadipogenic factor COUP-TF II (Fig. 6, D and E). Interestingly, NKX1-2 overexpression also inhibited the expression of Runx2, the master regulator of osteogenesis (62, 63), at Day 2 of ST2 adipocyte differentiation, whereas NKX1-2HDD had no effect on Runx2 expression (Fig. 6D). These findings suggest that NKX1-2 may inhibit the differentiation of ST2 cells into osteoblasts in addition to promoting their differentiation into adipocytes.

### Stable NKX1-2 overexpression inhibits ST2 cell osteoblastogenesis

Mesenchymal stem cells give rise to numerous cell types, including adipocytes and osteoblasts, and the mouse bone marrow-derived ST2 mesenchymal stromal cell line also can be differentiated into either of these cell types (64, 65). Because overexpression of NKX1-2 inhibited expression of Runx2, the master regulator of osteogenesis, at Day 2 of ST2 cell differentiation into adipocytes (Fig. 6D), we tested whether NKX1-2 also inhibits ST2 cell osteoblastogenesis. Thus, we analyzed the effect of stable overexpression of NKX1-2 when ST2 cells were induced to osteoblastogenic differentiation. Overexpression of NKX1-2 inhibited ST2 cell differentiation into osteoblasts, as evidenced by decreased staining for matrix mineralization with Alizarin Red (Fig. 7A) and decreased expression of the osteoblast markers osterix, alkaline phosphatase, and osteocalcin (Fig. 7B). In addition, there was a trend toward reduced expression of tyrosine-rich amelogenin peptide and receptor activator of NF- $\kappa$ B ligand. In contrast, the expression of Twist1 and Runx2 was unchanged. The lack of a decrease in Runx2 could reflect the fact that these analyses were performed at the end of osteoblastic differentiation (Day 18), by which time Runx2 expression has naturally declined. However, in additional experiments, we found that NKX1-2 overexpression also did not affect Runx2 expression at Days 6 and 10 of differentiation (data not shown). Overall, these results indicate that NKX1-2 regulates the bipotential ST2 cell toward an adipocyte cell fate and away from an osteoblast cell fate. However, the mechanism by which osteoblastogenesis is inhibited is unknown.

### Activation of the canonical Wnt pathway does not induce Nkx1-2 mRNA expression

Expression of Nkx1-2 mRNA is induced in P19 mouse embryonal carcinoma cells by inhibitors of glycogen synthase kinase 3 (GSK3) (40). Because GSK3 inhibitors activate canonical Wnt signaling, this provides evidence that, in P19 cells, Wnt induces Nkx1-2 mRNA. However, this induction could be a GSK3 inhibitor effect independent of Wnt or could be specific

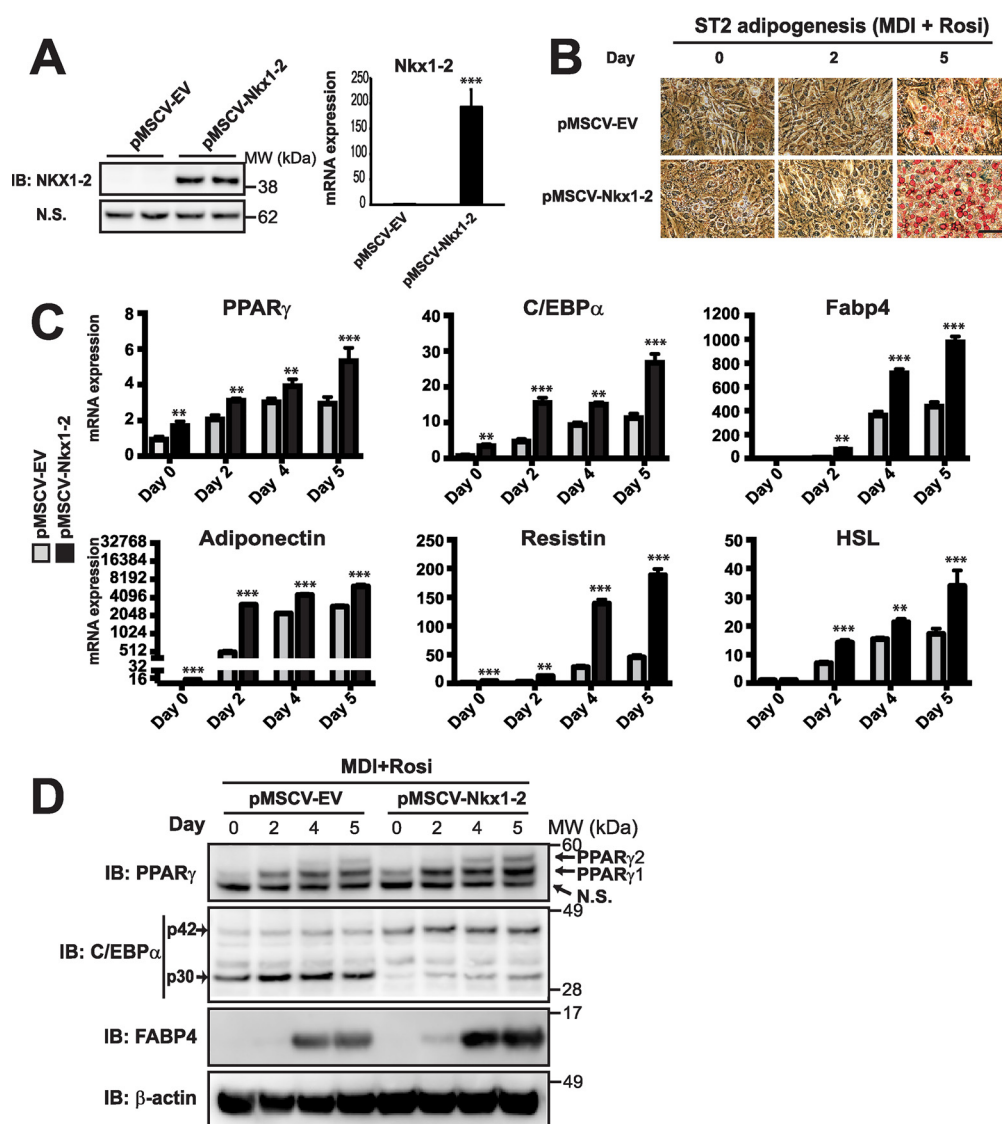


**Figure 4. Ectopic expression of NKX1-2 promotes adipocyte differentiation of ST2 cells.** *A*, left panel, immunoblotting (IB) for NKX1-2 was performed to assess protein expression in either empty vector control (pMSCV-EV) or NKX1-2–overexpressing undifferentiated ST2 cells (pMSCV-Nkx1-2). *N.S.*, a nonspecific band. *Right panel*, RT-qPCR analysis was performed to assess Nkx1-2 mRNA expression in pMSCV-EV or pMSCV-Nkx1-2 undifferentiated ST2 cells. Expression is normalized to cyclophilin, with expression in the empty vector cells set at 1. Data are presented as the mean  $\pm$  S.D. (error bars) of triplicate samples. Statistical significance *versus* empty vector was evaluated with the Student’s *t* test: \*\*\*,  $p < 0.001$ . *B*, pMSCV-EV or pMSCV-Nkx1-2 ST2 cells were induced to differentiate to adipocytes with the hormone mixture MDI + rosiglitazone (Rosi). Cells at the indicated time points after addition of the hormone mixture were stained with Oil Red O to assess neutral lipid accumulation. All panels are the same magnification; a 100- $\mu$ m scale bar is shown in the lower right panel. *C*, ST2 cells expressing pMSCV-EV or pMSCV-Nkx1-2 were induced to differentiate as in *B*, and RNA was harvested at the indicated time points. The expression of PPAR $\gamma$ , C/EBP $\alpha$ , Fabp4, adiponectin, resistin, and HSL was analyzed at the mRNA level by RT-qPCR. Data were normalized to cyclophilin, and expression of each gene at Day 0 in pMSCV-EV was set to 1; note that adiponectin expression is presented on a log scale. Data are presented as the mean  $\pm$  S.D. (error bars) of triplicate samples. Statistical significance *versus* empty vector double shControl was evaluated at each time point with the Student’s *t* test: \*\*,  $p < 0.01$  and \*\*\*,  $p < 0.001$ . These results are representative of three independent experiments. *D*, immunoblotting for adipocyte marker proteins PPAR $\gamma$ , C/EBP $\alpha$ , and FABP4 was performed at the time points indicated in pMSCV-EV and pMSCV-Nkx1-2 ST2 cells.  $\beta$ -Actin served as a loading control. *N.S.*, nonspecific band.

to P19 cells. Because canonical Wnt signaling inhibits adipogenesis (66) but NKX1-2 is proadipogenic, Wnt induction of Nkx1-2 mRNA would seem counterintuitive in adipogenic model systems. To evaluate whether the canonical Wnt pathway induces Nkx1-2 mRNA expression in a preadipocyte cell model, we treated primary mesenchymal stem cells isolated from mouse ears with recombinant mouse Wnt3a (Fig. 8). Expression of Axin2, a known canonical Wnt target, was induced  $\sim$ 100-fold at 4 h, whereas Nkx1-2 expression remained unchanged. At 24 h of Wnt3a treatment, Axin2 expression returned to baseline, and Nkx1-2 mRNA levels were

slightly repressed. These data indicate that canonical Wnt signaling does not induce Nkx1-2 expression in EMSCs. Although the mechanism of the slight repression of Nkx1-2 expression with 24 h of exposure to Wnt3a is unknown and may be indirect, this repression is consistent with the fact that Wnt3a is antiadipogenic and Nkx1-2 is proadipogenic.

## Discussion

Adipogenic differentiation of 3T3-L1 preadipocytes is sequentially controlled by two waves of transcriptional networks (67), with cross-talk between TFs and activating histone

## NKX1-2 regulates adipogenesis

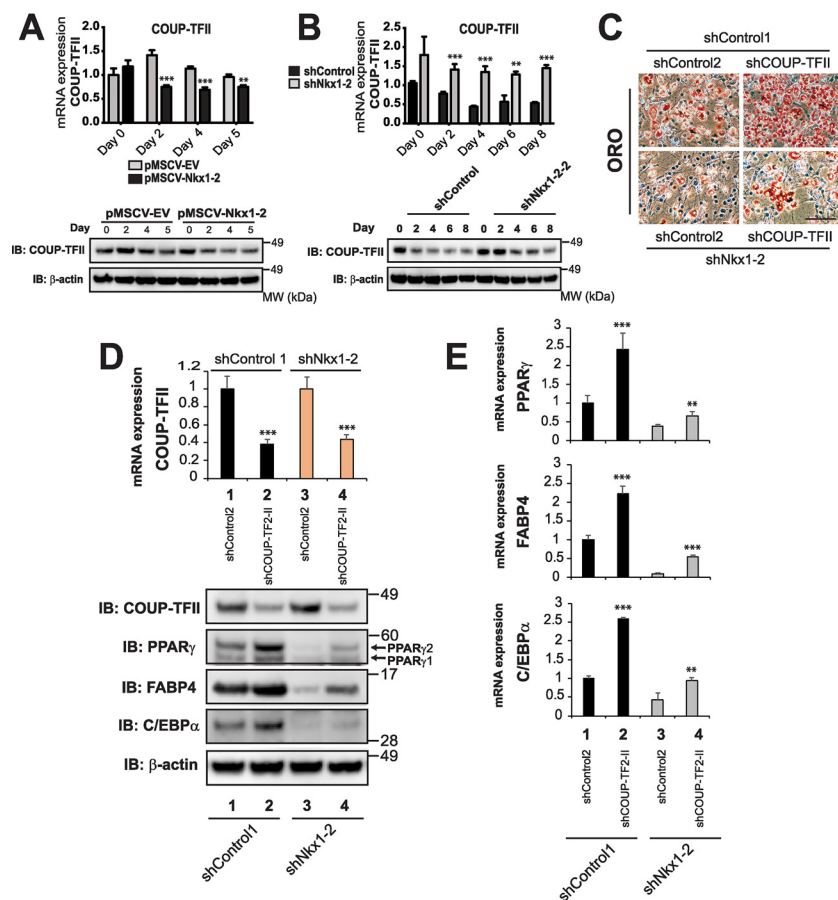


**Figure 5. NKX1-2 inhibits COUP-TF II expression during adipocyte differentiation of ST2 cells.** *A*, upper panel, RT-qPCR was performed to examine endogenous COUP-TF II mRNA expression in pMSCV-EV and pMSCV-Nkx1-2 ST2 cells during adipocyte differentiation following addition of the hormone mixture MDI + Rosi at Day 0. Data were normalized to cyclophilin, and expression of COUP-TF II at Day 0 in pMSCV-EV was set to 1. Data are given as the mean  $\pm$  S.D. (error bars) of triplicate samples. Statistical significance versus empty vector was evaluated at each time point with the Student's *t* test: \*\*,  $p < 0.01$  and \*\*\*,  $p < 0.001$ . The results are representative of three independent experiments. *A*, lower panel, immunoblotting (IB) was performed for COUP-TF II protein from cell lysates harvested as described in the upper panel.  $\beta$ -Actin served as a loading control. *B*, upper panel, RT-qPCR was performed to examine endogenous COUP-TF II mRNA expression in shControl and shNkx1-2 3T3-L1 cells during adipocyte differentiation after addition of the hormone mixture MDI. Data were normalized to cyclophilin, and expression of COUP-TF II at Day 0 in shControl was set to 1. Data are given as the mean  $\pm$  S.D. (error bars) of triplicate samples. Statistical significance versus shControl was evaluated at each time point with the Student's *t* test: \*\*,  $p < 0.01$  and \*\*\*,  $p < 0.001$ . The results are representative of three independent experiments. *B*, lower panel, immunoblotting was performed for COUP-TF II protein from cell lysates harvested as described in the upper panel.  $\beta$ -Actin served as a loading control. *C–E*, as indicated in Fig. 2, shControl (here defined as shControl 1) and shNkx1-2 3T3-L1 preadipocytes were further infected with either shControl (defined as shControl 2) or shCOUP-TF II expression vectors followed by adipocyte differentiation induced by MDI (as described in Fig. 2) up to Day 8. *C*, cells were stained with ORO to assess neutral lipid accumulation. All panels are the same magnification; a 100- $\mu$ m scale bar is shown in the lower right panel. *D*, upper panel, RT-qPCR was performed to examine endogenous COUP-TF II mRNA expression. Lower panel, immunoblotting was performed using the antibodies indicated. *E*, RT-qPCR was performed to examine adipocyte gene expression. For *D* and *E*, data were normalized to cyclophilin, and expression of COUP-TF II, PPAR $\gamma$ , FABP4, or C/EBP $\alpha$  p30 in double shControls was set to 1. Data are given as the mean  $\pm$  S.D. (error bars) of triplicate samples. Statistical significance versus double shControl was evaluated at each time point with the Student's *t* test: \*\*,  $p < 0.01$  and \*\*\*,  $p < 0.001$ . The results are representative of three independent experiments.

marks (8). Upon exposure to an adipogenic mixture, the first wave of TFs includes C/EBP $\beta/\delta$ , glucocorticoid receptor, and STAT5A. These factors then activate a second wave of TFs, including PPAR $\gamma$  and C/EBP $\alpha$ , that play the most prominent roles in terminal adipocyte differentiation. However, additional TFs are involved, and it is likely that others have yet to be discovered. In the present study, we found that NKX1-2 is induced during 3T3-L1 adipogenesis, whereas other NKX family members are not induced (Fig. 1). NKX1-2 has not been associated previously with adipose biology. Importantly, depletion of NKX1-2 by shRNAs in 3T3-L1 preadipocytes and mouse EMSCs inhibits their differentiation into mature adipocytes, as assessed both by decreased neutral lipid accumulation and decreased expression of mature adipocyte marker genes (Figs. 2 and 3). Reciprocally, ectopic expression of NKX1-2 in ST2 mes-

enchymal precursor cells promotes their adipogenic differentiation, again assessed both by lipid accumulation and marker gene expression (Fig. 4). These effects require that the NKX1-2 homeodomain (DNA-binding domain) be intact (Fig. 6), suggesting that NKX1-2 acts via direct interaction with its target DNA. Interestingly, ectopic expression of NKX1-2 up-regulates expression of the p42 isoform of C/EBP $\alpha$  protein but decreases expression of the p30 isoform (Figs. 4 and 6). These isoforms are derived from alternative translation start sites (58, 68), suggesting that NKX1-2 may regulate alternative translation to favor the p42 isoform (in addition to inducing expression of the C/EBP $\alpha$  mRNA). Previous reports showed that p42 C/EBP $\alpha$ , but not p30, has antimitotic activity and that p42 is sufficient to trigger the differentiation program of 3T3-L1 preadipocytes (57, 58). Therefore, our data suggest that selective induction of

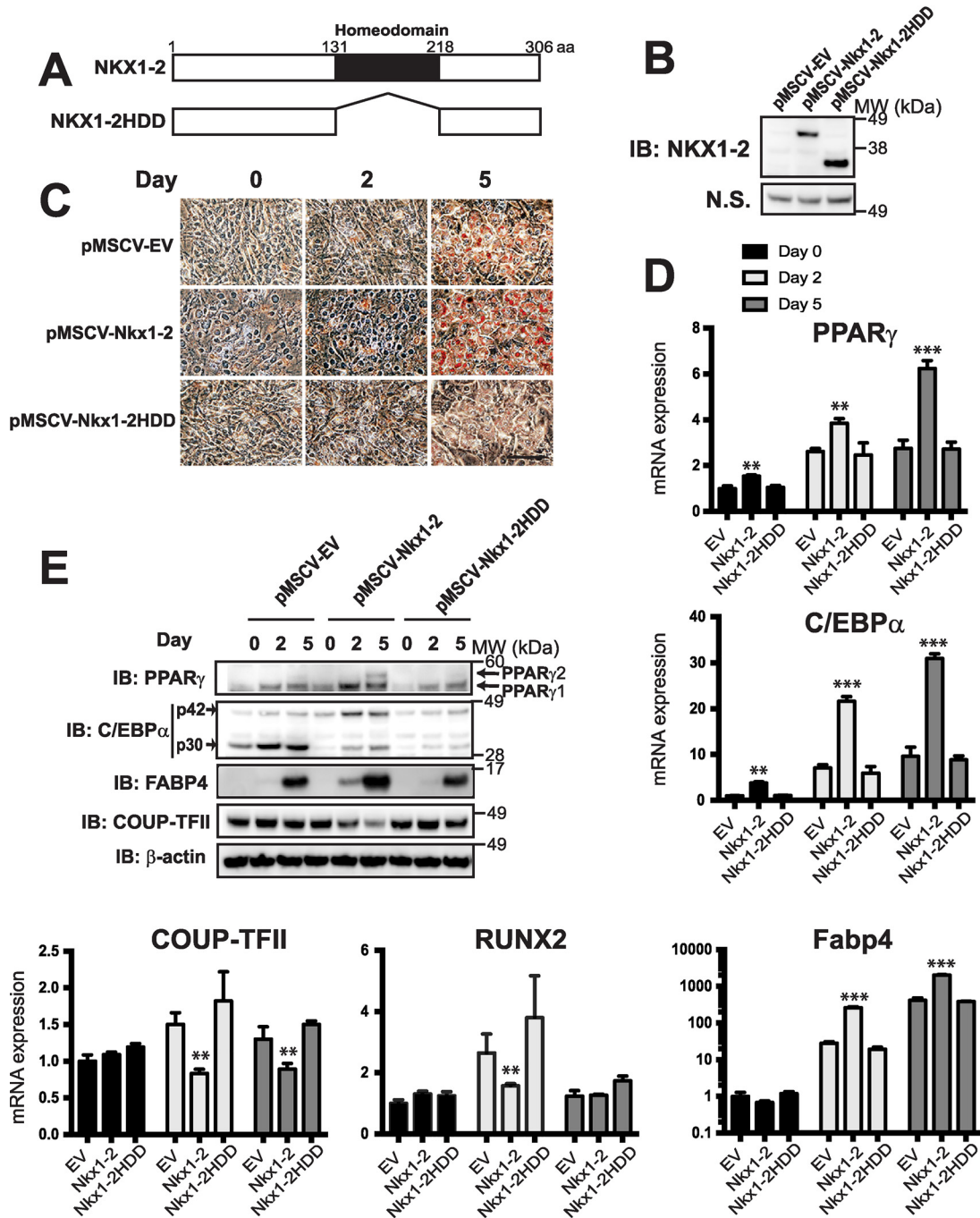


**Figure 6. The DNA-binding HD of NKX1-2 is required to promote adipocyte differentiation.** *A*, schematic presentation of the full-length NKX1-2 and its HD deletion mutant NKX1-2HDD. *B*, immunoblot using NKX1-2 antibody to confirm the overexpression of pMSCV-Nkx1-2 full-length protein and pMSCV-Nkx1-2HDD protein. *N.S.*, nonspecific band served as a loading control. *C*, pMSCV-EV, pMSCV-Nkx1-2, or pMSCV-Nkx1-2HDD ST2 cells were induced to differentiate to adipocytes by the hormone mixture MDI + Rosi. Cells were stained with Oil Red O to assess neutral lipid accumulation at the time points indicated (hormone mixture was added at Day 0). All panels are the same magnification; a 100- $\mu$ m scale bar is shown in the lower right panel. *D*, during adipocyte differentiation of pMSCV-EV, pMSCV-Nkx1-2, or pMSCV-Nkx1-2HDD ST2 cells with MDI + Rosi, RNA was harvested at the time points indicated, and the mRNA expression of PPAR $\gamma$ , C/EBP $\alpha$ , Fabp4, COUP-TF II, and Runx2 was analyzed by RT-qPCR. Data were normalized to cyclophilin, and expression of each gene at Day 0 in pMSCV-EV was set to 1; note that Fabp4 expression is on a log scale. Data are given as the mean  $\pm$  S.D. (error bars) of triplicate samples. Statistical significance was evaluated with an ANOVA followed by Dunnett's test compared with expression level of empty vector (EV) as control at each time point: \*\*,  $p < 0.01$  and \*\*\*,  $p < 0.001$ . The results are representative of three independent experiments. *E*, immunoblotting (IB) for adipocyte marker proteins PPAR $\gamma$ , C/EBP $\alpha$ , and FABP4 as well as COUP-TF II was performed on lysates harvested at the indicated time points of differentiation with MDI + Rosi.  $\beta$ -Actin served as a loading control.

the p42 C/EBP $\alpha$  isoform by NKX1-2 may be an important component of its proadipogenic action. However, depletion of NKX1-2 by shRNAs in 3T3-L1 preadipocytes decreases the expression of both the p42 and p30 isoforms of C/EBP $\alpha$  (Figs. 2 and S2), suggesting that the ability of NKX1-2 to

regulate the alternative translation of C/EBP $\alpha$  may be dose- or cell type-dependent.

Because PPAR $\gamma$  and C/EBP $\alpha$  are master proadipogenic TFs (9, 67, 69–74), regulation of their expression is a potentially powerful mechanism to regulate adipocyte differentiation. As



## NKX1-2 regulates adipogenesis

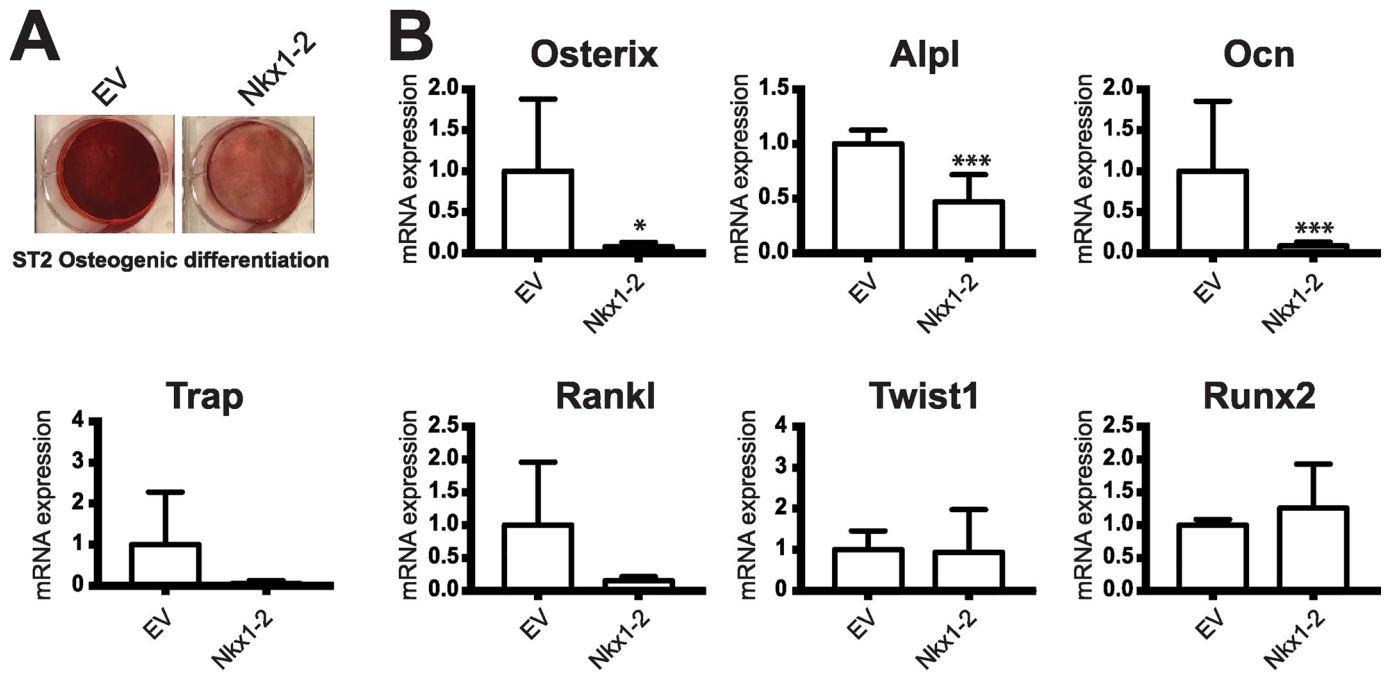


**Figure 7. Stable NKX1-2 overexpression inhibits ST2 cell osteoblastogenesis.** ST2 cells overexpressing NKX1-2 or empty vector control ST2 cells were differentiated for 18 days to promote osteoblastogenesis. *A*, matrix mineralization was stained using Alizarin Red. *B*, mRNA expression of osteogenic genes osterix, alkaline phosphatase (*Alpl*), osteocalcin (*Ocn*), tyrosine-rich amelogenin peptide (*Trap*), receptor activator of NF- $\kappa$ B ligand (*Rankl*), Twist Family BHLH Transcription Factor 1 (*Twist1*), and RUNX Family Transcription Factor 2 (*Runx2*) was analyzed by RT-qPCR. Transcripts were normalized to the geometric mean of TATA-binding protein, hypoxanthine-guanine phosphoribosyltransferase, ribosomal protein L32, and 18S rRNA and are presented as mean  $\pm$  S.D. (error bars) from six individual wells from one differentiation experiment. Two additional differentiation experiments demonstrated similar results in osteoblast marker expression and Alizarin Red staining. Statistical analysis was performed using a Student's *t* test: \*,  $p < 0.05$  and \*\*\*,  $p < 0.001$ .

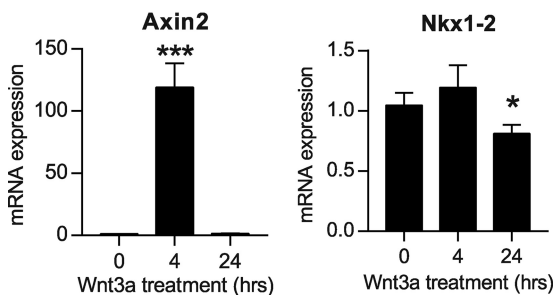


**Figure 8. Activation of the canonical Wnt pathway does not induce Nkx1-2 mRNA expression.** Confluent EMSCs were treated with 10 ng/ml recombinant mouse Wnt3a for 0, 4, or 24 h before harvest and RNA isolation ( $n = 6$  wells/group). mRNA expression of Axin2, a known canonical Wnt target, and Nkx1-2 was evaluated by RT-qPCR. Data were normalized to cyclophilin, and the expression of each gene at 0 h of Wnt3a treatment was set at 1. Data are given as the mean  $\pm$  S.D. (error bars). Statistical significance was evaluated with an ANOVA followed by Dunnett's test compared with the expression level at 0 h of Wnt3a treatment: \*,  $p < 0.05$  and \*\*\*,  $p < 0.001$ .

such, the antiadipogenic effect of COUP-TF II has been shown to be either downstream of Wnt/ $\beta$ -catenin via recruitment of the SMRT corepressor complex to the *Pparg* gene (55) or downstream of hedgehog signaling by association with GATA2 to repress the *Cepba* gene (56). Our data indicate that NKX1-2, which itself is a transcriptional repressor (40), negatively regulates the expression of COUP-TF II (Fig. 5), suggesting that the proadipogenic action of NKX1-2 is mediated at least in part by this mechanism. Interestingly, overexpression of NKX1-2 in ST2 cells only represses COUP-TF II expression after addition of the differentiation mixture; it does not affect the basal level of COUP-TF II at Day 0 (Figs. 5 and 6). However, overexpression of NKX1-2 does cause a small increase in the basal levels of

PPAR $\gamma$  and C/EBP $\alpha$  at Day 0 before addition of the differentiation mixture, suggesting that the mechanisms by which NKX1-2 up-regulates PPAR $\gamma$  and C/EBP $\alpha$  at Day 0 and during the differentiation may differ.

Bone marrow mesenchymal stromal cells can differentiate into adipocytes or osteoblasts, and, over time, excess differentiation toward adipocytes can lead to osteoporosis (75, 76). ST2 cells, which are a murine bone marrow-derived mesenchymal stromal cell line, also can differentiate along adipocyte or osteoblast lineages when cultured with appropriate mixtures (64, 65). Our data indicate that, in addition to enhancing ST2 cell differentiation in response to an adipogenic mixture, NKX1-2 inhibits ST2 cell differentiation in response to an osteoblastogenic mixture (Fig. 7). This suggests that NKX2-1 may play a role in the cell fate determination of bone marrow mesenchymal stromal cells and hence may play a role in the development of osteoporosis.

The molecular mechanisms underlying how NKX1-2 regulates differentiation toward adipocytes and away from osteoblasts remain to be fully defined. Fig. 9 presents a model based upon the current data, taking into account that NKX1-2 is a direct transcriptional repressor (40) and that the regulatory effects described here are lost upon deletion of the homeodomain. In this model, NKX1-2 is proadipogenic because it represses expression of COUP-TF II, which otherwise represses PPAR $\gamma$  and C/EBP $\alpha$ . The model shows that other, currently unknown mechanisms also may contribute to the proadipogenic effect. We initially hypothesized that NKX1-2 is antiosteoblastogenic due to repression of Runx2, a critical proosteoblastogenic factor. However, we found no evidence

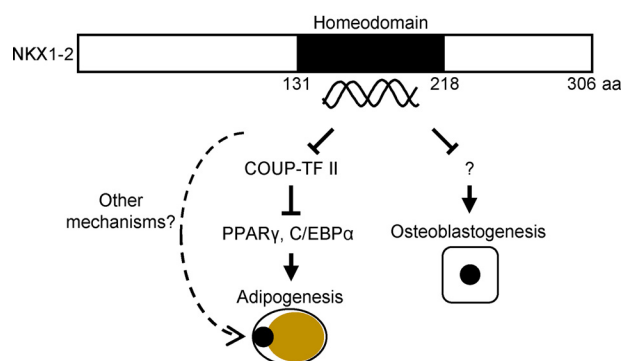


**Figure 9. Model of NKX1-2 regulation of adipogenic and osteoblastogenic differentiation.** NKX1-2 binds to target DNA via its homeodomain and functions as a transcriptional repressor. In a precursor cell (not shown), to promote adipogenesis it represses expression of COUP-TF II, which would otherwise repress the expression of the key proadipogenic transcription factors PPAR $\gamma$  and C/EBP $\alpha$ . Other mechanisms also may be involved, as indicated by the *dashed arrow*. The target of NKX1-2 that leads to repression of osteoblastogenesis is unknown, signified by a *question mark*. The adipocyte schematic shows stored lipid (yellow) and an eccentric nucleus (black). The osteoblast schematic shows a centrally located nucleus (black). aa, amino acids.

for NKX1-2-mediated repression of Runx2 during osteoblastogenic differentiation. Therefore, the model shows this mechanism as being unknown. In addition to exploring this model in depth, future studies should address the expression and role of NKX1-2 *in vivo*, both in normal human physiology and in pathological states such as osteoporosis.

## Experimental procedures

### Cell culture, staining, and reagents

Mouse 3T3-L1 preadipocytes and human embryonic kidney 293T cells were maintained in Dulbecco's modified Eagle's medium supplemented with 10% calf serum and penicillin-streptomycin at 37 °C in 10% CO<sub>2</sub>. Mouse marrow-derived ST2 cells were incubated at 37 °C in 5% CO<sub>2</sub> in  $\alpha$ -minimal essential medium supplemented with 10% FBS and penicillin-streptomycin. Induction of 3T3-L1 or ST2 cell differentiation was achieved by treatment of 2-day postconfluent cells (Day 0) in media supplemented with 10% FBS and a hormone mixture containing 3-isobutyl-1-methylxanthine (0.5 mM), dexamethasone (1  $\mu$ M), and insulin (0.167  $\mu$ M), denoted MDI. On Day 2, the cells were treated again with 0.167  $\mu$ M insulin and subsequently were refed with growth medium containing 10% FBS every 2 days. In some studies, pioglitazone or rosiglitazone (50 mM in DMSO) was added to the hormone mixture to achieve a final media concentration of 5  $\mu$ M (MDIP or MDIR). EMSCs, isolated from C57BL/6J mice as described previously (77, 78), were maintained in 5% CO<sub>2</sub> and Dulbecco's modified Eagle's medium/F-12 (1:1) media supplemented with 15% FBS and 10 ng/ml recombinant bFGF (PeproTech). To induce adipocyte differentiation, the media supplements were changed to 15% FBS and MDI without bFGF. Lipid accumulation in adipocytes was visualized by staining with ORO. Briefly, differentiated adipocytes were washed with phosphate-buffered saline (PBS) and fixed with 10% formaldehyde in PBS for 4 min. After two washes with water, cells were stained for 1–2 h with ORO working solution (0.3% (w/v) in 60% isopropanol). To induce osteoblastogenesis, ST2 cells were grown to confluence and fed with

osteogenic medium (ST2 medium supplemented with 10 mM  $\beta$ -glycerophosphate, 25  $\mu$ g/ml ascorbic acid 2-phosphate, and 3  $\mu$ M CHIR99021) (Stemgent) from Day 0 to Day 6 of differentiation. For Days 7–18 of differentiation, ST2 cells were cultured in the osteogenic medium in the absence of CHIR99021 (79) as described previously (80). Cells were fed with fresh osteogenic medium every 2 days thereafter. The degree of mineralization in osteoblasts was determined with 2% Alizarin Red staining at Day 18 postdifferentiation as described previously (80). The stain was aspirated, and cells were washed at least twice with water and photographed. To evaluate whether the Wnt pathway induces NKX1-2 expression, confluent EMSCs were treated with 10 ng/ml recombinant mouse Wnt3a (R&D Systems, Minneapolis, MN) for 0, 4, or 24 h. After the respective treatment period, cells were lysed in 1 ml of RNA Stat-60 (Tel Test, Alvin, TX) for RNA extraction and downstream qPCR analysis.

Antibodies against the following proteins were obtained as indicated: PPAR $\gamma$  (H-100, sc-7196), C/EBP $\alpha$  (14AA, sc-61), GAPDH (6C5, sc-32233), and NKX2-1/TTF-1 (H190, sc-13040) from Santa Cruz Biotechnology; FABP4 (catalog number MAB1443) from R&D Systems, Inc.; NKX1-2 (ab105940) from Abcam;  $\beta$ -actin (catalog number 4967), COUP-TF II (catalog number 6434), and HA-Tag (C29F4, catalog number 3724) from Cell Signaling Technology.

### Plasmids, transfection, retroviral infection, and reporter gene assays

The retroviral expression vector pMSCV-HA-TTF-1 (denoted as pMSCV-TTF-1) was described previously (54). The mouse NKX1-2 expression vector in pEF/nuc/myc (pEF-Nkx1-2-Myc) was kindly provided by Y. Marikawa (University of Hawaii, Honolulu, HI). To create the retroviral expression vector pMSCV-Nkx1-2-Myc, the PCR product of Nkx1-2 cDNA with EcoRI and BglII overhangs was purified and ligated to pMSCV (80) that had been digested with EcoRI and BglII. To construct pMSCV-Nkx1-2 with its HD deleted (pMSCV-Nkx1-2HDD), inverse PCR was used to delete NKX1-2 amino acids 131–218. For retroviral infection, 293T cells were transfected by calcium phosphate coprecipitation with pMSCV-EV, pMSCV-TTF-1, pMSCV-Nkx1-2, or pMSCV-Nkx1-2HDD retroviral expression vectors and viral packaging vectors as described previously (81). The virus-containing media were collected and applied to subconfluent 3T3-L1 or ST2 cells followed by 2  $\mu$ g/ml puromycin selection 72 h postinfection.

### shRNA knockdown of NKX1-2 and COUP-TF II

Knockdown of NKX1-2 in mouse 3T3-L1 cells and EMSCs was performed by infection with a lentivirus expressing either of two shRNAs targeting exon1 or -2 of Nkx1-2 or an shControl. Two different Mission lentivirus-based plasmids of shRNAs (clone numbers TRCN0000084835 and TRCN0000084836) against mouse Nkx1-2 and the shControl vector TRC2 pLKO.5-puro nonmammalian shRNA (SHC202) were obtained from Sigma-Aldrich. 293T cells were cotransfected with the shRNA and packaging plasmids psPAX2 and pMD2 by the calcium phosphate method to produce the lentivirus as described previously (81). To knock down COUP-TF II in shControl (shControl 1) or

## NKX1-2 regulates adipogenesis

shNkx1-2 3T3-L1 preadipocytes, shControl 2 (non-mammalian shRNA in pLKO.1-CMV-neo) or shCOUP-TF II (TRCN0000026167 in pLKO.1-CMV-neo), both obtained from Sigma-Aldrich, was cotransfected with packaging plasmids in 293T cells as described above, and the resulting lentivirus was used to infect shControl (shControl 1) and shNkx1-2 3T3-L1 preadipocytes, respectively.

### Cell lysis and immunoblotting

Cells were lysed in buffer containing 40 mM HEPES (pH 8.0), 120 mM sodium chloride, 10 mM sodium pyrophosphate, 10 mM sodium glycerophosphate, 1 mM EDTA, 50 mM sodium fluoride, 0.5 mM sodium orthovanadate, 1% Triton X-100, and protease inhibitor mixture tablets (catalog number 11836170001, Roche Applied Science). Cell lysates were gently resuspended and incubated at 4 °C with gentle rocking for 40 min to 1 h followed by microcentrifugation for 10 min at 4 °C. The supernatants were transferred to new tubes, and protein concentrations were determined. Proteins were separated by SDS-PAGE and transferred onto polyvinylidene difluoride membranes, and immunoblotting was performed using the antibodies described above. The primary and secondary antibodies were diluted with Signal Enhancer HIKAR Solution 1 and Solution 2, respectively, as described previously (54). Detection by enhanced chemiluminescence was with a SuperSignal West Dura kit (Thermo Fisher Scientific) and a Bio-Rad Fluor-S Max Multimager.

### RNA isolation and RT-qPCR

Total RNA was isolated with an RNeasy Mini kit (Qiagen, catalog number 74104) according to the manufacturer's instructions. Four micrograms of total RNA were reverse transcribed in 20- $\mu$ l total volume using the SuperScript III First Strand Synthesis System (catalog number 18080051, Thermo Scientific), and real-time qPCR was performed on the cDNA from 30 ng of RNA on a StepOnePlus Real-Time PCR System (Applied Biosystems) as described previously (81). Primer sequences used for qPCR are provided in Table S1.

### Statistical analysis

Results are presented as the mean  $\pm$  S.D. When comparing two groups, significance was determined using Student's *t* test. When multiple experimental groups were compared with a single control group, an analysis of variance (ANOVA) was followed by Dunnett's test. Significance is indicated as  $p < 0.05$  (\*),  $p < 0.01$  (\*\*), and  $p < 0.001$  (\*\*\*)

---

**Author contributions**—N. C., R. L. S., M. O., K. X., D. P. B., and B. X. formal analysis; N. C., R. L. S., M. O., K. X., D. P. B., O. A. M., R. J. K., and B. X. investigation; N. C., R. L. S., M. O., D. P. B., O. A. M., R. J. K., and B. X. methodology; D. P. B. and B. X. writing—original draft; D. P. B., O. A. M., R. J. K., and B. X. writing—review and editing; O. A. M., R. J. K., and B. X. conceptualization; O. A. M. and B. X. supervision; B. X. validation; B. X. visualization; B. X. project administration.

---

**Acknowledgment**—We thank Hiroyuki Mori for helping isolate EMSCs.

### References

1. Bornfeldt, K. E., and Tabas, I. (2011) Insulin resistance, hyperglycemia, and atherosclerosis. *Cell Metab.* **14**, 575–585 [CrossRef Medline](#)
2. Cristancho, A. G., and Lazar, M. A. (2011) Forming functional fat: a growing understanding of adipocyte differentiation. *Nat. Rev. Mol. Cell Biol.* **12**, 722–734 [CrossRef Medline](#)
3. Rosen, E. D., and MacDougald, O. A. (2006) Adipocyte differentiation from the inside out. *Nat. Rev. Mol. Cell Biol.* **7**, 885–896 [CrossRef Medline](#)
4. Harms, M., and Seale, P. (2013) Brown and beige fat: development, function and therapeutic potential. *Nat. Med.* **19**, 1252–1263 [CrossRef Medline](#)
5. Green, H., and Kehinde, O. (1975) An established preadipose cell line and its differentiation in culture. II. Factors affecting the adipose conversion. *Cell* **5**, 19–27 [CrossRef Medline](#)
6. Green, H., and Meuth, M. (1974) An established pre-adipose cell line and its differentiation in culture. *Cell* **3**, 127–133 [CrossRef Medline](#)
7. Lefterova, M. I., and Lazar, M. A. (2009) New developments in adipogenesis. *Trends Endocrinol. Metab.* **20**, 107–114 [CrossRef Medline](#)
8. Siersbæk, R., Nielsen, R., and Mandrup, S. (2012) Transcriptional networks and chromatin remodeling controlling adipogenesis. *Trends Endocrinol. Metab.* **23**, 56–64 [CrossRef Medline](#)
9. Farmer, S. R. (2006) Transcriptional control of adipocyte formation. *Cell Metab.* **4**, 263–273 [CrossRef Medline](#)
10. Li, D., Yea, S., Li, S., Chen, Z., Narla, G., Banck, M., Laborda, J., Tan, S., Friedman, J. M., Friedman, S. L., and Walsh, M. J. (2005) Kruppel-like factor-6 promotes preadipocyte differentiation through histone deacetylase 3-dependent repression of DLK1. *J. Biol. Chem.* **280**, 26941–26952 [CrossRef Medline](#)
11. Oishi, Y., Manabe, I., Tobe, K., Tsushima, K., Shindo, T., Fujiu, K., Nishimura, G., Maemura, K., Yamauchi, T., Kubota, N., Suzuki, R., Kitamura, T., Akira, S., Kadowaki, T., and Nagai, R. (2005) Kruppel-like transcription factor KLF5 is a key regulator of adipocyte differentiation. *Cell Metab.* **1**, 27–39 [CrossRef Medline](#)
12. Floyd, Z. E., and Stephens, J. M. (2003) STAT5A promotes adipogenesis in nonprecursor cells and associates with the glucocorticoid receptor during adipocyte differentiation. *Diabetes* **52**, 308–314 [CrossRef Medline](#)
13. Nanbu-Wakao, R., Morikawa, Y., Matsumura, I., Masuho, Y., Muramatsu, M. A., Senba, E., and Wakao, H. (2002) Stimulation of 3T3-L1 adipogenesis by signal transducer and activator of transcription 5. *Mol. Endocrinol.* **16**, 1565–1576 [CrossRef Medline](#)
14. Monteiro, M. C., Sanyal, M., Cleary, M. L., Sengenès, C., Bouloumié, A., Dani, C., and Billon, N. (2011) PBX1: a novel stage-specific regulator of adipocyte development. *Stem Cells* **29**, 1837–1848 [CrossRef Medline](#)
15. Chen, Z., Torrens, J. L., Anand, A., Spiegelman, B. M., and Friedman, J. M. (2005) Krox20 stimulates adipogenesis via C/EBP $\beta$ -dependent and -independent mechanisms. *Cell Metab.* **1**, 93–106 [CrossRef Medline](#)
16. Distel, R. J., Ro, H. S., Rosen, B. S., Groves, D. L., and Spiegelman, B. M. (1987) Nucleoprotein complexes that regulate gene expression in adipocyte differentiation: direct participation of *c-fos*. *Cell* **49**, 835–844 [CrossRef Medline](#)
17. White, U. A., and Stephens, J. M. (2010) Transcriptional factors that promote formation of white adipose tissue. *Mol. Cell. Endocrinol.* **318**, 10–14 [CrossRef Medline](#)
18. Maekawa, T., Jin, W., and Ishii, S. (2010) The role of ATF-2 family transcription factors in adipocyte differentiation: antiobesity effects of p38 inhibitors. *Mol. Cell. Biol.* **30**, 613–625 [CrossRef Medline](#)
19. Tong, Q., Dalgin, G., Xu, H., Ting, C. N., Leiden, J. M., and Hotamisligil, G. S. (2000) Function of GATA transcription factors in preadipocyte-adipocyte transition. *Science* **290**, 134–138 [CrossRef Medline](#)
20. Tong, Q., Tsai, J., Tan, G., Dalgin, G., and Hotamisligil, G. S. (2005) Interaction between GATA and the C/EBP family of transcription factors is critical in GATA-mediated suppression of adipocyte differentiation. *Mol. Cell. Biol.* **25**, 706–715 [CrossRef Medline](#)
21. Guermah, M., Ge, K., Chiang, C. M., and Roeder, R. G. (2003) The TBN protein, which is essential for early embryonic mouse development, is an inducible TAFII implicated in adipogenesis. *Mol. Cell* **12**, 991–1001 [CrossRef Medline](#)

22. Ge, K., Cho, Y. W., Guo, H., Hong, T. B., Guermah, M., Ito, M., Yu, H., Kalkum, M., and Roeder, R. G. (2008) Alternative mechanisms by which mediator subunit MED1/TRAP220 regulates peroxisome proliferator-activated receptor  $\gamma$ -stimulated adipogenesis and target gene expression. *Mol. Cell. Biol.* **28**, 1081–1091 [CrossRef Medline](#)
23. Grøntved, L., Madsen, M. S., Boergesen, M., Roeder, R. G., and Mandrup, S. (2010) MED14 tethers mediator to the N-terminal domain of peroxisome proliferator-activated receptor  $\gamma$  and is required for full transcriptional activity and adipogenesis. *Mol. Cell. Biol.* **30**, 2155–2169 [CrossRef Medline](#)
24. Wang, W., Huang, L., Huang, Y., Yin, J. W., Berk, A. J., Friedman, J. M., and Wang, G. (2009) Mediator MED23 links insulin signaling to the adipogenesis transcription cascade. *Dev. Cell* **16**, 764–771 [CrossRef Medline](#)
25. Lefterova, M. I., Steger, D. J., Zhuo, D., Qatanani, M., Mullican, S. E., Tuteja, G., Manduchi, E., Grant, G. R., and Lazar, M. A. (2010) Cell-specific determinants of peroxisome proliferator-activated receptor  $\gamma$  function in adipocytes and macrophages. *Mol. Cell. Biol.* **30**, 2078–2089 [CrossRef Medline](#)
26. Lefterova, M. I., Zhang, Y., Steger, D. J., Schupp, M., Schug, J., Cristancho, A., Feng, D., Zhuo, D., Stoeckert, C. J., Jr., Liu, X. S., and Lazar, M. A. (2008) PPAR $\gamma$  and C/EBP factors orchestrate adipocyte biology via adjacent binding on a genome-wide scale. *Genes Dev.* **22**, 2941–2952 [CrossRef Medline](#)
27. Mikkelsen, T. S., Xu, Z., Zhang, X., Wang, L., Gimble, J. M., Lander, E. S., and Rosen, E. D. (2010) Comparative epigenomic analysis of murine and human adipogenesis. *Cell* **143**, 156–169 [CrossRef Medline](#)
28. Nielsen, R., Pedersen, T. A., Hagenbeek, D., Moulos, P., Siersbaek, R., Megens, E., Denissov, S., Børgesen, M., Francoijs, K. J., Mandrup, S., and Stunnenberg, H. G. (2008) Genome-wide profiling of PPAR $\gamma$ :RXR and RNA polymerase II occupancy reveals temporal activation of distinct metabolic pathways and changes in RXR dimer composition during adipogenesis. *Genes Dev.* **22**, 2953–2967 [CrossRef Medline](#)
29. Siersbæk, R., Baek, S., Rabiee, A., Nielsen, R., Traynor, S., Clark, N., Sandelin, A., Jensen, O. N., Sung, M. H., Hager, G. L., and Mandrup, S. (2014) Molecular architecture of transcription factor hotspots in early adipogenesis. *Cell Rep.* **7**, 1434–1442 [CrossRef Medline](#)
30. Siersbæk, R., Nielsen, R., John, S., Sung, M. H., Baek, S., Loft, A., Hager, G. L., and Mandrup, S. (2011) Extensive chromatin remodelling and establishment of transcription factor 'hotspots' during early adipogenesis. *EMBO J.* **30**, 1459–1472 [CrossRef Medline](#)
31. Siersbaek, R., Nielsen, R., and Mandrup, S. (2010) PPAR $\gamma$  in adipocyte differentiation and metabolism—novel insights from genome-wide studies. *FEBS Lett.* **584**, 3242–3249 [CrossRef Medline](#)
32. Siersbæk, R., Rabiee, A., Nielsen, R., Sidoli, S., Traynor, S., Loft, A., Poulsen, L. C., Rogowska-Wrzesinska, A., Jensen, O. N., and Mandrup, S. (2014) Transcription factor cooperativity in early adipogenic hotspots and super-enhancers. *Cell Rep.* **7**, 1443–1455 [CrossRef Medline](#)
33. Steger, D. J., Grant, G. R., Schupp, M., Tomaru, T., Lefterova, M. I., Schug, J., Manduchi, E., Stoeckert, C. J., Jr., and Lazar, M. A. (2010) Propagation of adipogenic signals through an epigenomic transition state. *Genes Dev.* **24**, 1035–1044 [CrossRef Medline](#)
34. Wakabayashi, K., Okamura, M., Tsutsumi, S., Nishikawa, N. S., Tanaka, T., Sakakibara, I., Kitakami, J., Ihara, S., Hashimoto, Y., Hamakubo, T., Kodama, T., Aburatani, H., and Sakai, J. (2009) The peroxisome proliferator-activated receptor  $\gamma$ /retinoid X receptor  $\alpha$  heterodimer targets the histone modification enzyme PR-Set7/Setd8 gene and regulates adipogenesis through a positive feedback loop. *Mol. Cell. Biol.* **29**, 3544–3555 [CrossRef Medline](#)
35. Muhr, J., Andersson, E., Persson, M., Jessell, T. M., and Ericson, J. (2001) Groucho-mediated transcriptional repression establishes progenitor cell pattern and neuronal fate in the ventral neural tube. *Cell* **104**, 861–873 [CrossRef Medline](#)
36. Papizan, J. B., Singer, R. A., Tschen, S. I., Dhawan, S., Friel, J. M., Hipkens, S. B., Magnuson, M. A., Bhushan, A., and Sussel, L. (2011) Nkx2.2 repressor complex regulates islet  $\beta$ -cell specification and prevents  $\beta$ -to- $\alpha$ -cell reprogramming. *Genes Dev.* **25**, 2291–2305 [CrossRef Medline](#)
37. Thangapazham, R., Saenz, F., Katta, S., Mohamed, A. A., Tan, S. H., Petrovics, G., Srivastava, S., and Dobi, A. (2014) Loss of the NKX3.1 tumor suppressor promotes the *TMPPRS2-ERG* fusion gene expression in prostate cancer. *BMC Cancer* **14**, 16 [CrossRef Medline](#)
38. Cunningham, T. J., Colas, A., and Duester, G. (2016) Early molecular events during retinoic acid induced differentiation of neuromesodermal progenitors. *Biol. Open* **5**, 1821–1833 [CrossRef Medline](#)
39. Rodrigo Albors, A., Halley, P. A., and Storey, K. G. (2018) Lineage tracing of axial progenitors using Nkx1-2CreER(T2) mice defines their trunk and tail contributions. *Development* **145**, dev164319 [CrossRef Medline](#)
40. Tamashiro, D. A., Alarcon, V. B., and Marikawa, Y. (2012) Nkx1-2 is a transcriptional repressor and is essential for the activation of Brachyury in P19 mouse embryonal carcinoma cell. *Differentiation* **83**, 282–292 [CrossRef Medline](#)
41. Simon, R., Britsch, S., and Bergemann, A. (2011) Ablation of *Sax2* gene expression prevents diet-induced obesity. *FEBS J.* **278**, 371–382 [CrossRef Medline](#)
42. Briscoe, J., Sussel, L., Serup, P., Hartigan-O'Connor, D., Jessell, T. M., Rubenstein, J. L., and Ericson, J. (1999) Homeobox gene *Nkx2.2* and specification of neuronal identity by graded Sonic hedgehog signalling. *Nature* **398**, 622–627 [CrossRef Medline](#)
43. Sussel, L., Kalamaras, J., Hartigan-O'Connor, D. J., Meneses, J. J., Pedersen, R. A., Rubenstein, J. L., and German, M. S. (1998) Mice lacking the homeodomain transcription factor Nkx2.2 have diabetes due to arrested differentiation of pancreatic  $\beta$  cells. *Development* **125**, 2213–2221 [Medline](#)
44. Fagman, H., and Nilsson, M. (2011) Morphogenetics of early thyroid development. *J. Mol. Endocrinol.* **46**, R33–R42 [CrossRef Medline](#)
45. Hadrys, T., Braun, T., Rinkwitz-Brandt, S., Arnold, H. H., and Bober, E. (1998) Nkx5-1 controls semicircular canal formation in the mouse inner ear. *Development* **125**, 33–39 [Medline](#)
46. Rinkwitz-Brandt, S., Arnold, H. H., and Bober, E. (1996) Regionalized expression of *Nkx5-1*, *Nkx5-2* and *sek* genes during mouse inner ear development. *Hear Res.* **99**, 129–138 [CrossRef Medline](#)
47. Taylor, B. L., Liu, F. F., and Sander, M. (2013) Nkx6.1 is essential for maintaining the functional state of pancreatic  $\beta$  cells. *Cell Rep.* **4**, 1262–1275 [CrossRef Medline](#)
48. Schaffer, A. E., Taylor, B. L., Benthuisen, J. R., Liu, J., Thorel, F., Yuan, W., Jiao, Y., Kaestner, K. H., Herrera, P. L., Magnuson, M. A., May, C. L., and Sander, M. (2013) Nkx6.1 controls a gene regulatory network required for establishing and maintaining pancreatic  $\beta$  cell identity. *PLoS Genet.* **9**, e1003274 [CrossRef Medline](#)
49. Chelban, V., Patel, N., Vandrovцова, J., Zanetti, M. N., Lynch, D. S., Ryten, M., Botia, J. A., Bello, O., Tribollet, E., Efthymiou, S., Davagnanam, I., SYNAPSE Study Group, Bashiri, F. A., Wood, N. W., Rothman, J. E., et al. (2017) Mutations in NKX6-2 cause progressive spastic ataxia and hypomyelination. *Am. J. Hum. Genet.* **100**, 969–977 [CrossRef Medline](#)
50. Kimura, S., Hara, Y., Pineau, T., Fernandez-Salguero, P., Fox, C. H., Ward, J. M., and Gonzalez, F. J. (1996) The T/ebp null mouse: thyroid-specific enhancer-binding protein is essential for the organogenesis of the thyroid, lung, ventral forebrain, and pituitary. *Genes Dev.* **10**, 60–69 [CrossRef Medline](#)
51. Yu, J., and Koenig, R. J. (2018) Thyroid-specific PPAR $\gamma$  deletion is benign in the mouse. *Endocrinology* **159**, 1463–1468 [CrossRef Medline](#)
52. Kroll, T. G., Sarraf, P., Pecciarini, L., Chen, C. J., Mueller, E., Spiegelman, B. M., and Fletcher, J. A. (2000) PAX8-PPAR $\gamma$ 1 fusion oncogene in human thyroid carcinoma. *Science* **289**, 1357–1360 [CrossRef Medline](#); Correction (2000) **289**, 1474
53. Dobson, M. E., Diallo-Krou, E., Grachtchouk, V., Yu, J., Colby, L. A., Wilkinson, J. E., Giordano, T. J., and Koenig, R. J. (2011) Pioglitazone induces a proadipogenic antitumor response in mice with PAX8-PPAR $\gamma$  fusion protein thyroid carcinoma. *Endocrinology* **152**, 4455–4465 [CrossRef Medline](#)
54. Xu, B., O'Donnell, M., O'Donnell, J., Yu, J., Zhang, Y., Sartor, M. A., and Koenig, R. J. (2016) Adipogenic differentiation of thyroid cancer cells through the Pax8-PPAR $\gamma$  fusion protein is regulated by thyroid transcription factor 1 (TTF-1). *J. Biol. Chem.* **291**, 19274–19286 [CrossRef Medline](#)
55. Okamura, M., Kudo, H., Wakabayashi, K., Tanaka, T., Nonaka, A., Uchida, A., Tsutsumi, S., Sakakibara, I., Naito, M., Osborne, T. F., Hamakubo, T., Ito, S., Aburatani, H., Yanagisawa, M., Kodama, T., et al. (2009) COUP-TFII acts downstream of Wnt/ $\beta$ -catenin signal to silence PPAR $\gamma$  gene

## NKX1-2 regulates adipogenesis

- expression and repress adipogenesis. *Proc. Natl. Acad. Sci. U.S.A.* **106**, 5819–5824 [CrossRef Medline](#)
56. Xu, Z., Yu, S., Hsu, C. H., Eguchi, J., and Rosen, E. D. (2008) The orphan nuclear receptor chicken ovalbumin upstream promoter-transcription factor II is a critical regulator of adipogenesis. *Proc. Natl. Acad. Sci. U.S.A.* **105**, 2421–2426 [CrossRef Medline](#)
57. Lin, F. T., and Lane, M. D. (1994) CCAAT/enhancer binding protein  $\alpha$  is sufficient to initiate the 3T3-L1 adipocyte differentiation program. *Proc. Natl. Acad. Sci. U.S.A.* **91**, 8757–8761 [CrossRef Medline](#)
58. Lin, F. T., MacDougald, O. A., Diehl, A. M., and Lane, M. D. (1993) A 30-kDa alternative translation product of the CCAAT/enhancer binding protein  $\alpha$  message: transcriptional activator lacking antimetabolic activity. *Proc. Natl. Acad. Sci. U.S.A.* **90**, 9606–9610 [CrossRef Medline](#)
59. Damante, G., Fabbro, D., Pellizzari, L., Civitareale, D., Guazzi, S., Polycarpou-Schwartz, M., Cauci, S., Quadrioglio, F., Formisano, S., and Di Lauro, R. (1994) Sequence-specific DNA recognition by the thyroid transcription factor-1 homeodomain. *Nucleic Acids Res.* **22**, 3075–3083 [CrossRef Medline](#)
60. Sessa, G., Morelli, G., and Ruberti, I. (1993) The Athb-1 and -2 HD-Zip domains homodimerize forming complexes of different DNA binding specificities. *EMBO J.* **12**, 3507–3517 [CrossRef Medline](#)
61. Freyd, G., Kim, S. K., and Horvitz, H. R. (1990) Novel cysteine-rich motif and homeodomain in the product of the *Caenorhabditis elegans* cell lineage gene *lin-11*. *Nature* **344**, 876–879 [CrossRef Medline](#)
62. Komori, T., Yagi, H., Nomura, S., Yamaguchi, A., Sasaki, K., Deguchi, K., Shimizu, Y., Bronson, R. T., Gao, Y. H., Inada, M., Sato, M., Okamoto, R., Kitamura, Y., Yoshiki, S., and Kishimoto, T. (1997) Targeted disruption of *Cbfa1* results in a complete lack of bone formation owing to maturational arrest of osteoblasts. *Cell* **89**, 755–764 [CrossRef Medline](#)
63. Ducy, P., Zhang, R., Geoffroy, V., Ridall, A. L., and Karsenty, G. (1997) *Osf2/Cbfa1*: a transcriptional activator of osteoblast differentiation. *Cell* **89**, 747–754 [CrossRef Medline](#)
64. Ding, J., Nagai, K., and Woo, J. T. (2003) Insulin-dependent adipogenesis in stromal ST2 cells derived from murine bone marrow. *Biosci. Biotechnol. Biochem.* **67**, 314–321 [CrossRef Medline](#)
65. Yamaguchi, A., Ishizuya, T., Kintou, N., Wada, Y., Katagiri, T., Wozney, J. M., Rosen, V., and Yoshiki, S. (1996) Effects of BMP-2, BMP-4, and BMP-6 on osteoblastic differentiation of bone marrow-derived stromal cell lines, ST2 and MC3T3-G2/PA6. *Biochem. Biophys. Res. Commun.* **220**, 366–371 [CrossRef Medline](#)
66. Ross, S. E., Hemati, N., Longo, K. A., Bennett, C. N., Lucas, P. C., Erickson, R. L., and MacDougald, O. A. (2000) Inhibition of adipogenesis by Wnt signaling. *Science* **289**, 950–953 [CrossRef Medline](#)
67. Lefterova, M. I., Haakonsson, A. K., Lazar, M. A., and Mandrup, S. (2014) PPAR $\gamma$  and the global map of adipogenesis and beyond. *Trends Endocrinol. Metab.* **25**, 293–302 [CrossRef Medline](#)
68. Ossipow, V., Descombes, P., and Schibler, U. (1993) CCAAT/enhancer-binding protein mRNA is translated into multiple proteins with different transcription activation potentials. *Proc. Natl. Acad. Sci. U.S.A.* **90**, 8219–8223 [CrossRef Medline](#)
69. Barak, Y., Nelson, M. C., Ong, E. S., Jones, Y. Z., Ruiz-Lozano, P., Chien, K. R., Koder, A., and Evans, R. M. (1999) PPAR $\gamma$  is required for placental, cardiac, and adipose tissue development. *Mol. Cell* **4**, 585–595 [CrossRef Medline](#)
70. El-Jack, A. K., Hamm, J. K., Pilch, P. F., and Farmer, S. R. (1999) Reconstitution of insulin-sensitive glucose transport in fibroblasts requires expression of both PPAR $\gamma$  and C/EBP $\alpha$ . *J. Biol. Chem.* **274**, 7946–7951 [CrossRef Medline](#)
71. Freytag, S. O., Paielli, D. L., and Gilbert, J. D. (1994) Ectopic expression of the CCAAT/enhancer-binding protein  $\alpha$  promotes the adipogenic program in a variety of mouse fibroblastic cells. *Genes Dev.* **8**, 1654–1663 [CrossRef Medline](#)
72. Rosen, E. D., Sarraf, P., Troy, A. E., Bradwin, G., Moore, K., Milstone, D. S., Spiegelman, B. M., and Mortensen, R. M. (1999) PPAR $\gamma$  is required for the differentiation of adipose tissue *in vivo* and *in vitro*. *Mol. Cell* **4**, 611–617 [CrossRef Medline](#)
73. Tontonoz, P., Hu, E., and Spiegelman, B. M. (1994) Stimulation of adipogenesis in fibroblasts by PPAR $\gamma$ 2, a lipid-activated transcription factor. *Cell* **79**, 1147–1156 [CrossRef Medline](#)
74. Wu, Z., Rosen, E. D., Brun, R., Hauser, S., Adelmant, G., Troy, A. E., McKeon, C., Darlington, G. J., and Spiegelman, B. M. (1999) Cross-regulation of C/EBP $\alpha$  and PPAR $\gamma$  controls the transcriptional pathway of adipogenesis and insulin sensitivity. *Mol. Cell* **3**, 151–158 [CrossRef Medline](#)
75. Nuttall, M. E., and Gimble, J. M. (2004) Controlling the balance between osteoblastogenesis and adipogenesis and the consequent therapeutic implications. *Curr. Opin. Pharmacol.* **4**, 290–294 [CrossRef Medline](#)
76. Pino, A. M., Rosen, C. J., and Rodríguez, J. P. (2012) In osteoporosis, differentiation of mesenchymal stem cells (MSCs) improves bone marrow adipogenesis. *Biol. Res.* **45**, 279–287 [CrossRef Medline](#)
77. Mori, H., Prestwich, T. C., Reid, M. A., Longo, K. A., Gerin, I., Cawthorn, W. P., Susulic, V. S., Krishnan, V., Greenfield, A., and Macdougald, O. A. (2012) Secreted frizzled-related protein 5 suppresses adipocyte mitochondrial metabolism through WNT inhibition. *J. Clin. Investig.* **122**, 2405–2416 [CrossRef Medline](#)
78. Rim, J. S., Mynatt, R. L., and Gawronska-Kozak, B. (2005) Mesenchymal stem cells from the outer ear: a novel adult stem cell model system for the study of adipogenesis. *FASEB J.* **19**, 1205–1207 [CrossRef Medline](#)
79. Bennett, C. N., Ross, S. E., Longo, K. A., Bajnok, L., Hemati, N., Johnson, K. W., Harrison, S. D., and MacDougald, O. A. (2002) Regulation of Wnt signaling during adipogenesis. *J. Biol. Chem.* **277**, 30998–31004 [CrossRef Medline](#)
80. Kang, S., Bennett, C. N., Gerin, I., Rapp, L. A., Hankenson, K. D., and Macdougald, O. A. (2007) Wnt signaling stimulates osteoblastogenesis of mesenchymal precursors by suppressing CCAAT/enhancer-binding protein  $\alpha$  and peroxisome proliferator-activated receptor  $\gamma$ . *J. Biol. Chem.* **282**, 14515–14524 [CrossRef Medline](#)
81. Xu, B., Gerin, I., Miao, H., Vu-Phan, D., Johnson, C. N., Xu, R., Chen, X. W., Cawthorn, W. P., MacDougald, O. A., and Koenig, R. J. (2010) Multiple roles for the non-coding RNA SRA in regulation of adipogenesis and insulin sensitivity. *PLoS One* **5**, e14199 [CrossRef Medline](#)